Mars Phoenix Entry, Descent, and Landing Simulation Design and Modelling Analysis

Jill L. Prince[1], Prasun N. Desai[2], and Eric M. Queen[3]
NASA Langley Research Center, Hampton VA 23681

Myron. R. Grover[4]
Jet Propulsion Laboratory, Pasadena, CA 91109

The 2007 Mars Phoenix Lander was launched in August of 2007 on a ten month cruise to reach the northern plains of Mars in May 2008. Its mission continues NASA's pursuit to find evidence of water on Mars. Phoenix carries upon it a slew of science instruments to study soil and ice samples from the northern region of the planet, an area previously undiscovered by robotic landers. In order for these science instruments to be useful, it was necessary for Phoenix to perform a safe entry, descent, and landing (EDL) onto the surface of Mars. The EDL design was defined through simulation and analysis of the various phases of the descent. An overview of the simulation and various models developed to characterize the EDL performance is provided. Monte Carlo statistical analysis was performed to assess the performance and robustness of the Phoenix EDL system and are presented in this paper. Using these simulation and modelling tools throughout the design and into the operations phase, the Mars Phoenix EDL was a success on May 25, 2008.

Nomenclature

A	=	spacecraft area
AoA	=	angle of attack
C_A	=	aerodynamic axial force coefficient
C_D	=	aerodynamic drag coefficient
C_{D0}	=	parachute aerodynamic drag coefficient
CG	=	center of gravity
C_{ll}	=	aerodynamic rolling moment
C_m	=	aerodynamic pitch moment coefficient
C_{mq}	=	aerodynamic pitch moment dynamic stability coefficient
C_N	=	aerodynamic normal force coefficient
C_n	=	aerodynamic yaw moment coefficient
C_{nr}	=	aerodynamic yaw moment dynamic stability coefficient
CSS	=	cruise stage separation
C_x	=	parachute opening load factor
C_Y	=	aerodynamic side force coefficient
D	=	diameter of aeroshell
D_0	=	parachute nominal diameter
E	=	atmospheric entry time
FPA	=	flight-path angle
G&C	=	guidance and control

[1]Aerospace Engineer, Atmospheric Flight & Entry Systems Branch, MS 489, jill.l.prince@nasa.gov, AIAA Member.
[2]Senior Aerospace Engineer, Atmospheric Flight & Entry Systems Branch, MS 489, prasun.n.desai@nasa.gov, AIAA Associate Fellow.
[3]Senior Aerospace Engineer, Atmospheric Flight & Entry Systems Branch, MS 489, eric.m.queen@nasa.gov, AIAA Member.
[4]Senior Aerospace Engineer, EDL Systems Advanced Technologies Group, 4800 Oak Grover Drive, MS 301-490, myron.r.grover@jpl.nasa.gov, AIAA Member.

Ixx, Iyy, Izz = principal moments of inertia
Ixy, Iyz, Ixz = cross products of inertia
Kn = Knudsen number
L = spacecraft landing time
L_B = parachute bridle length
L_R = parachute riser length
L_S = parachute suspension length
LS = lander separation
M = Mach number
n = exponent in parachute inflation model
q = dynamic pressure
RCS = reaction control system
S_0 = parachute nominal area
t = time
TCM = trajectory correction maneuver
t_{FI} = time at full inflation of the parachute
t_{LS} = time of line stretch of the parachute
t_{MF} = time of mortar firing
V_h = horizontal velocity
V_r = planet-relative entry velocity
V_v = vertical velocity
X_{cg} = axial CG location
Z_{cg} = lateral CG location
γ_r = planet-relative entry flight path angle

I. Introduction

IN August 2003, the Mars Phoenix was selected as the first Mars Scout mission. Borne of the cancelled 2001 Surveyor Lander, Phoenix was intended as the sister spacecraft of the Mars Polar Lander (MPL) that was lost in 1999.[1,2] Because there was not enough time to address findings of the MPL failure review prior to the 2001 launch window, the Surveyor mission was cancelled and the spacecraft was shelved until its reincarnation as Phoenix as a proposed Scout mission in 2003 for launch in 2007. The Phoenix spacecraft is the Surveyor spacecraft with modified science payloads. It was equipped with an enhanced radar, EDL communication system, and enhanced test program.[3,4]

The Phoenix mission to Mars was launched on August 4, 2007 beginning a 10-month cruise to the red planet. During the cruise and approach phases, four trajectory correction maneuvers (TCM) were performed to more closely target the designated landing site in the northern polar region. Once the spacecraft was on its nominal course, the seven minutes of entry, descent, and landing brought Phoenix through Mars' atmosphere and safely to the surface of Mars. This paper focuses on the entry, descent, and landing simulation and performance analysis of the Mars Phoenix mission.

The Phoenix simulation at NASA Langley Research Center (LaRC) was the prime simulation used for Monte Carlo analysis to assess the robustness of the EDL phase. Many groups, however, supported the development of the simulation of the EDL phase providing various models that were incorporated within it: the spacecraft team at Lockheed Martin Space Systems (LMSS) supplied the flight software models (e.g., parachute deploy algorithm, terminal descent guidance and control models); the Jet Propulsion Laboratory (JPL) team provided the radar model; the LaRC team provided the aerodynamics models (e.g., capsule, parachute, lander). In addition, much of the post-processing and analysis of the simulation was performed by the entire EDL simulation team consisting of engineers and analysts at LaRC, JPL, and LMSS. This critical analysis of the EDL phase led to a safe and successful landing of Phoenix on Mars on May 25, 2008.

II. EDL Overview – Phases of Flight

The EDL segment of the Phoenix mission begins as the spacecraft approaches the atmosphere and terminates with landing. The EDL simulation was modelled at LaRC from entry minus ten minutes until touchdown. After the ten-month cruise in anticipation for EDL, Phoenix separates from the cruise stage at entry minus seven minutes. After this separation and the slew to entry attitude, Phoenix enters the atmosphere at approximately 125 km radial altitude (radius of 3522.2 km). From atmospheric interface to parachute deploy, Phoenix relies on aerodynamic sta-

bility to traverse through the hypersonic phase (a phase extending the traditional definition of hypersonic in this scenario ending with parachute deploy at approximately Mach 1.6). Fifteen seconds after mortar fire of the parachute, the heatshield is jettisoned. Ten seconds following this event, the lander legs deploy. After radar activation and reacting to a terminal descent guidance algorithm, the lander separates from the backshell and parachute combination and soon thereafter performs a powered terminal descent to slow the lander to land safely on the surface of Mars. This EDL sequence of events is shown in Fig. 1.

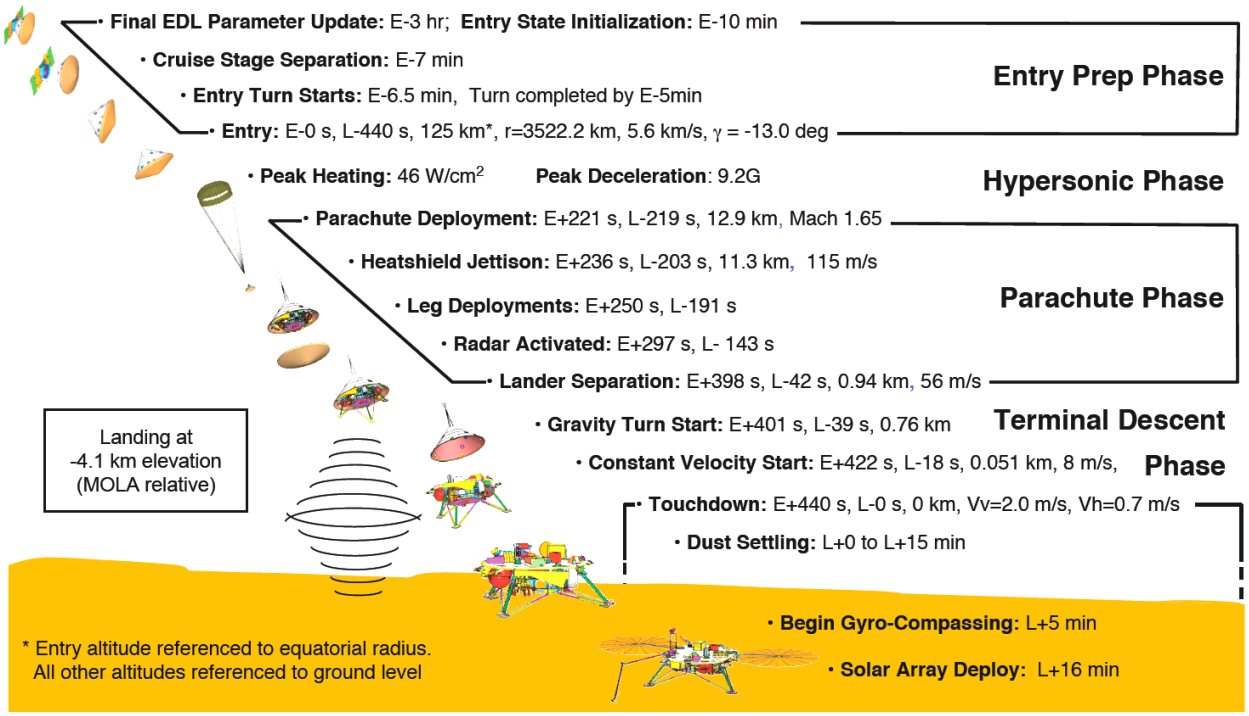

Figure 1. Phoenix EDL sequence of events.

A. Cruise Phase

The cruise phase of Phoenix began August 4, 2007 and continued until Mars atmospheric entry on May 25, 2008. During this phase, the health of the spacecraft was determined, and several trajectory correction maneuvers (TCM) were planned for landing site targeting.[5] The first TCM was performed 10 days after the launch from Kennedy Space Center, placing the spacecraft's trajectory in line with Mars. Later TCM's were planned to adjust the trajectory for better targeting. TCM-1, TCM-2, and TCM-3 were all executed close to nominal performance. Three weeks prior to landing, a TCM-4 was planned but cancelled. The trajectory at that time did not warrant the level of correction that TCM-4 would have provided. TCM-5 was performed nominally eight days prior to entry. A sixth and final TCM was planned for entry minus 21 hours but was called off because the nominal trajectory and the predicted landing ellipse at the time was safely within the landing region of interest. More information on the cruise phase of flight can be found in Ref. 5. Reference 6 provides an overview of the EDL analysis performed during the operations phase supporting the TCM design and landing site targeting.[6]

B. Hypersonic Phase

With the Phoenix launch at the beginning of the designated launch window, its inertial entry velocity was designed to enter the Mars atmosphere at 5.6 km/s at a -13.0° inertial entry flight path angle. This entry velocity is comparable to Mars Exploration Rovers (MER) at 5.5 km/s and between the entry velocities of Mars Pathfinder (7.6 km/s) and the Viking Landers (4.5 km/s). Additionally, the Phoenix Lander has nearly the same entry capsule configuration as MER and Mars Pathfinder as shown in Fig. 2. The forebody is a 70° sphere cone with a very similar aftbody. The mass of the Phoenix entry system was 572.7 kg, less massive than each MER and slightly more mas-

sive than the Mars Pathfinder. The ballistic coefficient of the Phoenix entry system was approximately 65 kg/m^2, comparable to Mars Pathfinder.

The hypersonic entry of the Phoenix entry capsule was originally planned to use a hypersonic guidance algorithm developed by NASA Johnson Space Center.[7] Because of timeline and budget constraints, and to reduce mission complexity, the hypersonic guidance was descoped in 2004. The Phoenix project considered a lift-up trajectory similar to the Viking entries. Because of the large landing footprints that a lift-up trajectory would incur (approximately 250 km), a change to a three-axis stabilized ballistic trajectory was made. This change reduced the footprint to approximately 100 km, within the science team requirement. However, late in 2006, analysis showed an interaction between the aerodynamic flowfield around the capsule and the thruster plumes from the reaction control system (RCS), which necessitated another change to the EDL entry mode.[8] It was determined that due to uncertainties in the performance of the RCS thrusters in this environment (the possibility existed of a control system instability), the deadbands within which the RCS thrusters would not fire were increased to large angles and rates, effectively turning off any hypersonic control of the vehicle. As such, Phoenix became the first ballistic non-spinning capsule without hypersonic thruster control to enter Mars. Reference 4 provides an overview of the evolution of the Phoenix EDL architecture.

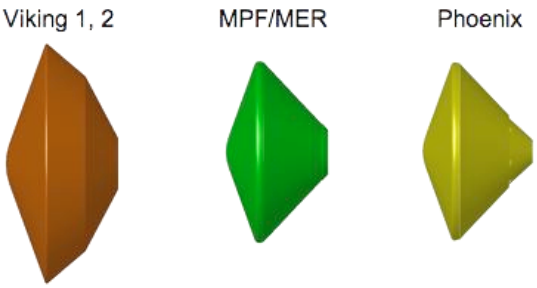

	Viking 1, 2	MPF/MER	Phoenix
Diameter, m	3.505	2.65	2.65
Relative Entry Velocity, (V_r), km/s	4.5, 4.42	7.6/5.5	5.6
Relative Entry FPA, (γ_r), deg	-17.6	-13.8/-11.5	-13.0
Entry Mass, kg	930	585/840	570
m/(C_DA), kg/m^2	63.7	62.3/89.8	62
X_{CG}/D reference	0.222	0.27	0.253
Z_{CG}/D reference	0.0132	0.0	0.0
G&C	3-axis (active)	spin stabilized	ballistic uncontrolled

Figure 2. Phoenix entry vehicle configuration relative to previous missions.

C. Parachute Phase

The parachute phase of EDL consists of the time between mortar-fire of the parachute to separation of the lander from the backshell-parachute system. Nominally, this phase takes approximately 173 seconds. The parachute is an 11.73-m diameter disk-gap-band parachute with Viking heritage. It is mortar-fired based on a trigger designed to contain parachute deploy within a Mach and dynamic pressure box. Nominally, mortar fire occurs at a dynamic pressure of 490 Pa and Mach 1.64 approximately 220 seconds after atmospheric entry. Parachute deployment occurs at a nominal altitude of 12.7 km above the surface.

Fifteen seconds after mortar fire, the heatshield is jettisoned from the lander system. In these 15 seconds, the Mach number has decreased from Mach 1.64 to 0.52 and the relative velocity has decreased from 370 m/s to 118 m/s. Ten seconds after the heatshield is jettisoned, the lander legs are deployed at approximately 10.1 km above the surface. At 980 m above the surface (145 seconds after heatshield jettison), the lander is separated from the backshell-parachute system. At this point, the lander is traveling at 54 m/s and because of the wrist-mode oscillation of the lander under the parachute, the nominal angle of attack of the vehicle has increased from 2.3° to 8.5°. Rates on the vehicle at lander separation have increased to 37 ± 65 deg/s. This estimation of capsule rates was performed with a wrist-mode algorithm developed by JPL and will be discussed in Subsection H. Separate calculations using a multi-body simulation have shown that these rates are conservative estimates. Multi-body simulation calculations have shown rates at lander separation of 12 ± 22 deg/s.[9]

D. Terminal Descent Phase

The events between lander separation and touchdown make up the terminal descent phase. Immediately after lander separation, a tip-up maneuver occurs. At this point, if the horizontal velocity is below a certain threshold, a Backshell Avoidance Maneuver (BAM) is performed (essentially a larger tip-up maneuver angle) moving the lander further in the upwind direction to maximize the distance between it and the backshell-parachute system to avoid recontact between the two bodies. The required distance between the lander and backshell at touchdown is 30 meters. After tip-up, the gravity turn phase begins followed by a constant velocity phase. At approximately 52 m above

the surface, the lander begins its final descent having a velocity between 2-2.4 m/s. The lander touches the surface of Mars (-4.1 km with respect to the MOLA areoid) with a vertical velocity of 2.1 m/s and a horizontal velocity less than 1.4 m/s. The propellant usage during the terminal descent phase is approximately 37.4 kg. Total fuel usage including cruise, hypersonic, and terminal descent usage nominally is 50 kg. Phoenix lands nominally at 68.2° N Latitude and 233.4° E Longitude.

III. Modelling

The simulation used at LaRC for the Phoenix trajectory analyses was the Program to Optimize Simulated Trajectories 2 (POST II). This program is a six-degree-of-freedom (6DOF) simulation with multi-vehicle capabilities utilized for the modelling of the entry capsule, heatshield, backshell, parachute, and lander during EDL. This program has vast heritage in previous EDL flight experiences.[10,11,12] Several Phoenix specific models have been developed to accurately simulate the EDL phase of Phoenix. Models implemented into trajectory simulation during the hypersonic phase include IMU, atmosphere, and aerodynamics models. The parachute phase involves a parachute deployment algorithm and inflation model. These parachute models along with a parachute drag model are required to accurately predict the opening loads on the parachute as well as to the lander itself. Wind models and atmosphere models significantly impact the effect of the parachute and lander interaction with the Mars environment. In the final phase of EDL, parachute wrist-mode model, the radar model, terminal descent guidance, and propulsive control model are the more important contributions to the success of EDL. In addition, several spacecraft component interaction models are necessary to predict 6DOF flight from entry to landing. Some of these EDL models are discussed in detail in subsequent sections.

E. Atmosphere and Wind Modelling

Several sets of 2000 atmosphere profiles have been developed specifically for the Phoenix landing sites and season incorporating day-to-day variations in temperature and pressure. These profiles include regional density, temperature, and pressure characteristics with respect to altitude. The atmospheric representations provided include modelling of near surface temperatures using a mesoscale model. For much of the development phase of EDL, the atmospheric density model used was based on Mars Global Surveyor Thermal Emission Spectrometer (TES) temperature profiles for the Phoenix landing box of 65°-72° north latitudes and averaged about the entire longitudinal band. These TES profiles were taken near 2:00 pm local time and were extrapolated to a wider range of local times using Mars Regional Atmospheric Modelling System (MRAMS) and global climate models to accommodate EDL. Surface pressure and surface temperature from one-dimensional models were also incorporated to create the density profiles. These density profiles were enhanced with global climate model output. Figure 3 shows the percentage difference of the 2000 individual profiles from the nominal density profile.[13] A variation of ±20% is seen between 40-70 km, a ±10% variation between 20-40 km, less than ±5% variation between 3-10 km, and ±15% variation near the surface.

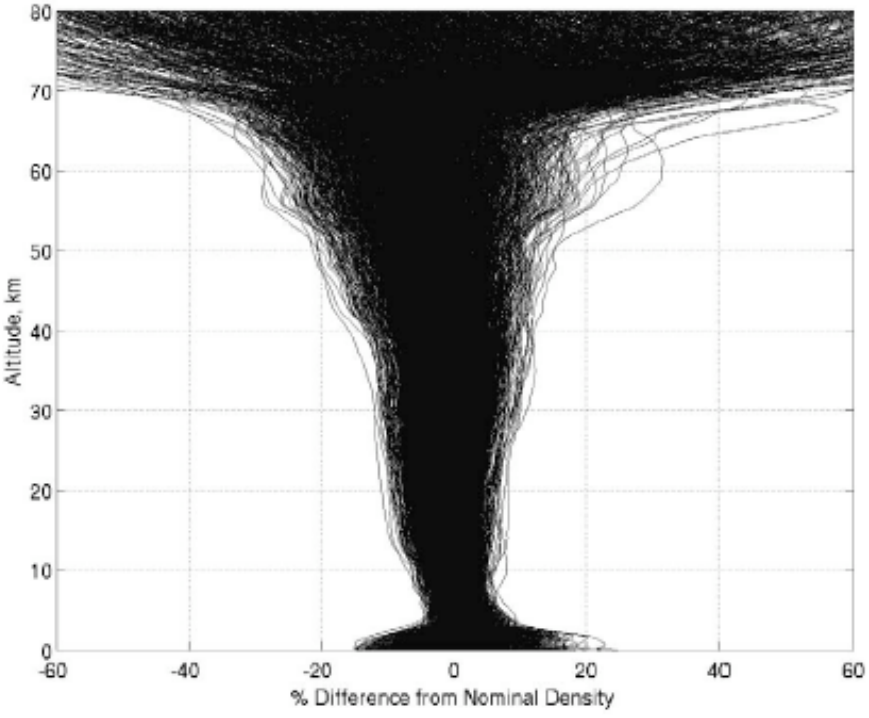

Figure 3. Ratio of density profiles to nominal density profile.

A driving condition of performance during the parachute phase is the effect of regional winds. The inclusions of winds can increase lander separation altitude, separation velocity, and fuel usage. Sets of 2000 Phoenix EDL Atmospheric Model (PEDLAM) winds were developed for the Phoenix landing sites and season. These wind profiles were estimated using mesoscale and Large Eddy Simulation (LES) models to estimate winds at a variety of Mars conditions.[13] These wind profiles have significant speeds and high frequency data up to 24 km above the surface as shown in Figs. 4 and 5. Vertical winds are typically upwards of ±20 m/s until 7 km above the surface, then the winds taper off to within ±5 m/s at higher altitudes. Most horizontal winds speeds average approximately 5-10 m/s throughout the altitude range of interest. Approximately 10% of the wind profiles are outlier wind profiles and can have horizontal velocities twice as large as the typical horizontal wind, as shown in Fig. 5.

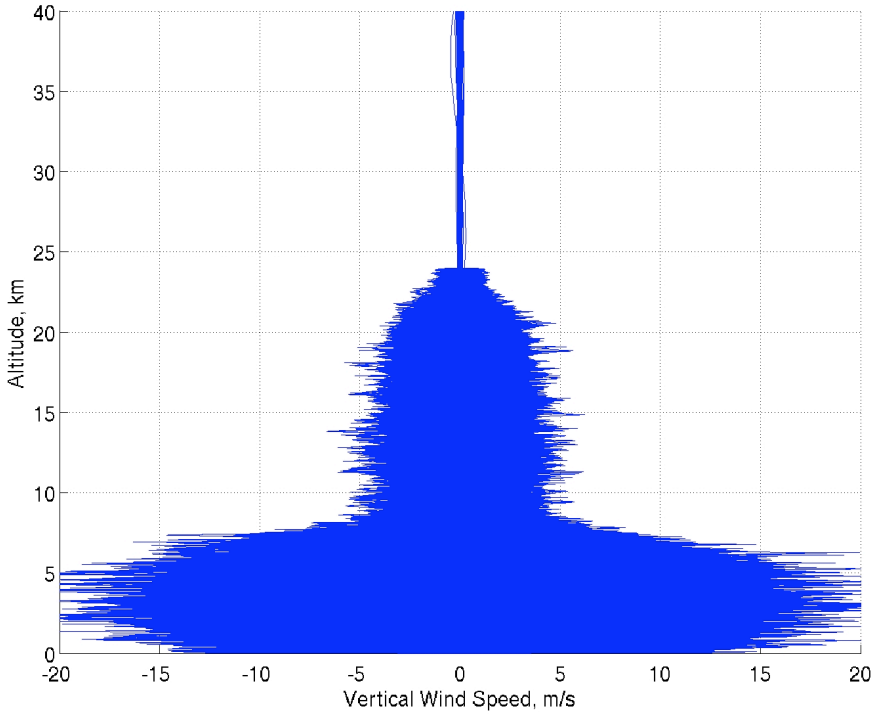

Figure 4. Vertical wind profiles.

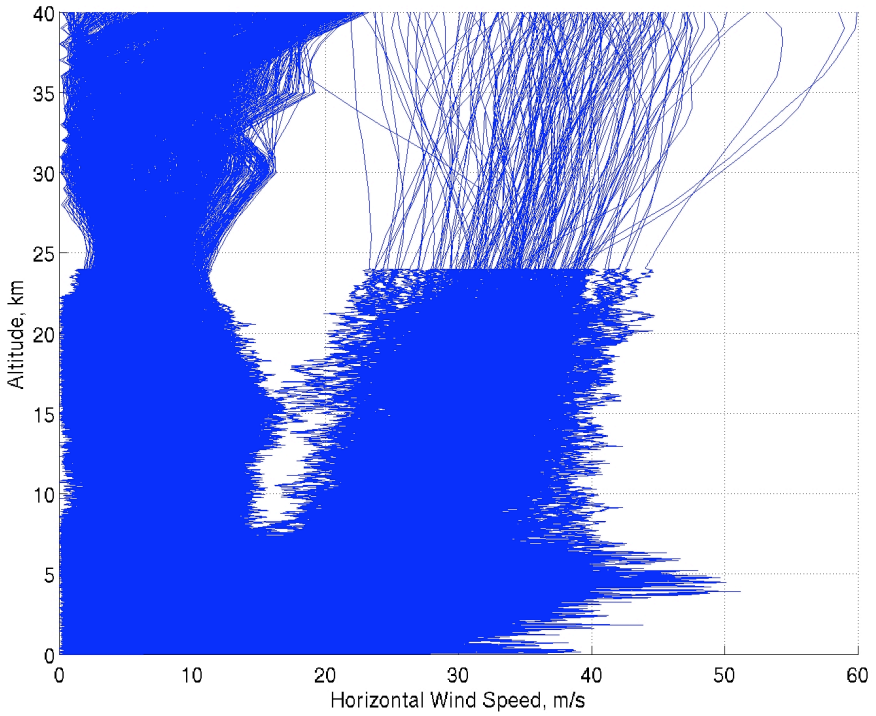

Figure 5. Horizontal wind profiles.

F. Aerodynamics

The Phoenix simulation consists of several aerodynamic databases to support its various configurations throughout EDL. First, the hypersonic aerodynamic database is constructed from the experience of the previous Mars entry vehicles: Mars Exploration Rovers (MER), Mars Pathfinder, and Viking.[14] The Phoenix entry velocity was 5.6 km/s; its trajectory follows a similar path of the previous MER entries, shown in Fig. 6.

The aero database consists of normal, axial, and side force coefficients, pitching and yawing moment coefficients, and pitch and yaw dynamic damping coefficients for a specified range of angles of attack and velocity or Knudsen number. Building on the successful missions of Viking, Mars Pathfinder, and MER, several enhancements were made for the Phoenix entry. More data points and an improved computational grid were used. For Mach numbers

between 0.4 and 1.5, Viking wind tunnel data were incorporated. Also, modifications to the dynamic damping coefficient uncertainties were made to more accurately represent the Phoenix entry. Reference 14 provides an in-depth description of the capsule aerodynamics.

G. Parachute Drag, Inflation

Parachute deployment was triggered on accelerometer measurements from an IMU, and was nominally targeted for acceleration value of 7.8 m/s^2, which corresponded to a dynamic pressure of 490 N/m^2. The parachute used during the Phoenix EDL is a Viking-type Disk-Gap-Band parachute 11.73 m in diameter. The drag model of the parachute was based on Viking parachute wind tunnel data, Viking Balloon Launched Decelerator Test (BLDT) program data, and Viking flight data.[15] An uncertainty of ±15% is uniformly placed on this nominal drag profile. This drag model is shown in Fig 7.

In addition to the parachute drag model, an empirical inflation model is incorporated into the POST simulation.

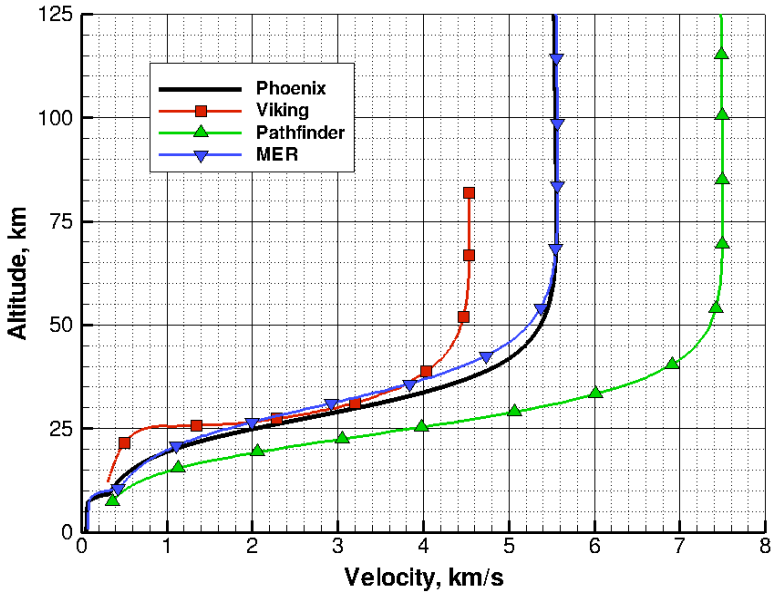

Figure 6. Phoenix entry trajectory relative to MER, Mars Pathfinder.

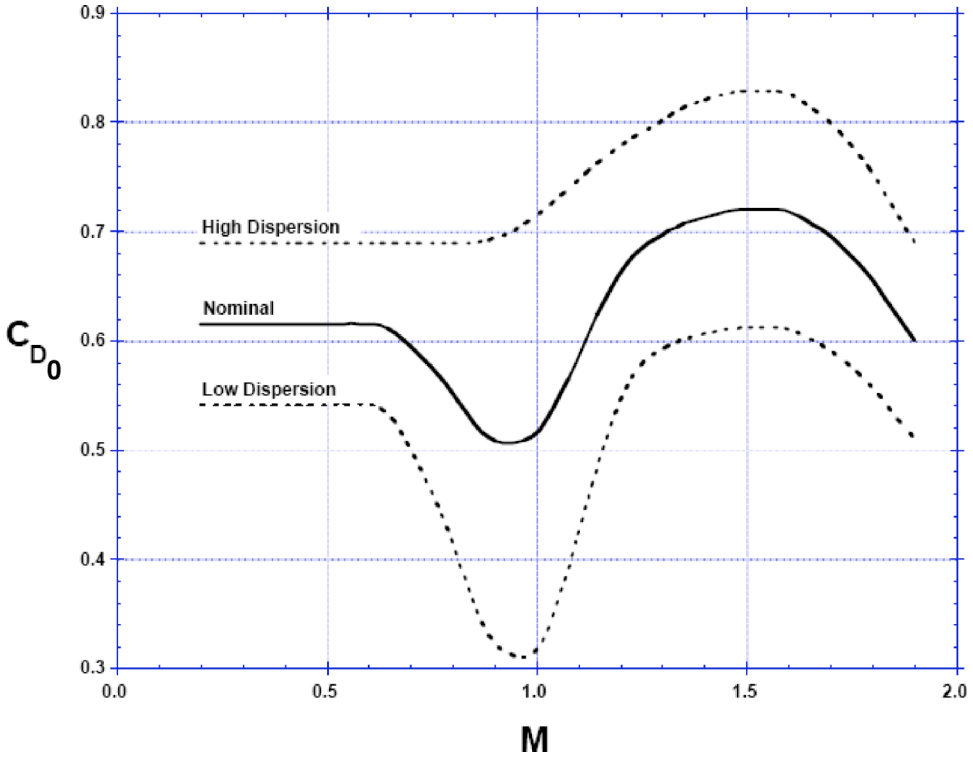

Figure 7. Phoenix parachute drag model with upper and lower bounds.

This inflation model provides first-order peak opening load information and accurate force histories for EDL analysis. This inflation model is calibrated and validated against Viking BLDT and flight data, Pathfinder, and MER flight data. The deployment time (time of line stretch, t_{LS}) is modelled as

$$t_{LS} = t_{MF} + \frac{L_B + L_R + L_S}{29.4} \tag{1}$$

where t_{MF} is the time of mortar firing, L_B, L_R, and L_S are the lengths of the bridle line, riser line, and suspension lines, respectively. During the time from mortar fire to full line stretch, the drag from the parachute is zero. The time of full inflation is defined as

$$t_{FI} = t_{LS} + \frac{D_0}{27.2} \tag{2}$$

where D_0 is the nominal diameter of the parachute. During the time of inflation, from full line stretch to full inflation, the drag force from the parachute is modelled as

$$F_P = qC_{D0}S_0C_x\left(\frac{t - t_{LS}}{t_{FI} - t_{LS}}\right)^n \tag{3}$$

where q is the dynamic pressure, C_{D0} is the parachute drag coefficient given in Fig. 7, S_0 is the parachute area, C_x is the opening load factor (1.344 in this case), and n is the exponent in the inflation model (4 in this case). Further details of the parachute drag and inflation model can be found in Ref. 15.

H. Parachute Wrist-Mode Model

After the parachute is deployed, the capsule hanging underneath will experience relatively large angles and rates arising from the parachute deployment process. To account for this two-body dynamical interaction between the parachute and capsule in the POST II EDL simulation, a simplified single-body nonlinear wrist-mode model was developed to conservatively estimate the torques on the capsule arising from the parachute dynamics. The simplified model is based on the assumption of a rigid statically determinant triple riser, although the algorithm has logic that mimics bridle-line slack and tension in the system. The model relies upon the parachute drag vector and the capsule CG position. The geometry of the system (the confluence point position and the triple bridle attachment points) is assumed internally. When the single bridle loading angle is less than or equal to half the triple bridle cone angle, all three triple bridle lines remain in tension. If the loading angle exceeds half of the triple bridle angle, then one or two of the triple bridle legs may go slack. The wrist-mode model outputs the resulting torque about the capsule CG and the number of slack bridle lines to the POST II program. This single-body wrist mode model was developed for computational expediency for the EDL simulation. However, a multi-body Phoenix simulation was developed in an effort to determine more realistic parachute/capsule dynamics and is the subject of Ref. 9.

IV. Performance Metrics

I. Nominal Entry Trajectory

The Phoenix EDL trajectory analysis begins with states ten minutes prior to entry. During these ten minutes, the spacecraft separates from its cruise stage and begins a slew to entry attitude. The spacecraft enters the atmosphere at a –13º inertial flight-path angle. Once the spacecraft achieves noticeable deceleration (0.03 g) the attitude control deadbands are enlarged to allow significant attitude excursions prior to parachute deploy. The increase in the attitude deadbands is the result of the aforementioned analysis of the interaction between the aerodynamic flowfield and the RCS thrusters plumes during hypersonic flight.[8] Even with little to no RCS control during the hypersonic phase, the stability of the Phoenix during flight nominally achieves approximately three degrees in total angle of attack (AoA)

at parachute deploy. The nominal attitude profile is shown in Fig 8. The first two peaks in angle of attack (occurring at approximately 75 s and 125 s) arise from bounded aerodynamic static instabilities, which are described in Ref. 14.

Predictions on the nominal Phoenix trajectory show that the maximum heating is well within specified requirements. A peak heat rate value of 46 W/cm^2 and a deceleration of 9.1 Earth g is shown in the nominal trajectory during the hypersonic phase. The total integrated heat load of the nominal hypersonic profile is 2400 J/cm^2.

Requirements on the angle of attack at parachute deploy limit the attitude that the capsule can attain. Attitudes greater than 10° lead to a 100 deg/s wrist-mode rate at lander separation for an instantaneously applied parachute flight limit load. This situation would impact radar performance, as well as the tip-up maneuver during terminal descent. As such, attitudes greater than 10° were of concern. The maximum deployment angle of attack demonstrated during the Viking BLDT test program was 13°. Attitudes greater than 15° would exceed the 100 deg/s wrist-mode rate at lander separation with realistic parachute load time histories. If the angle of attack exceeds 20º, there is a risk to the parachute inflation. The Monte Carlo results of the attitude of the spacecraft at parachute deploy is detailed is the next section.

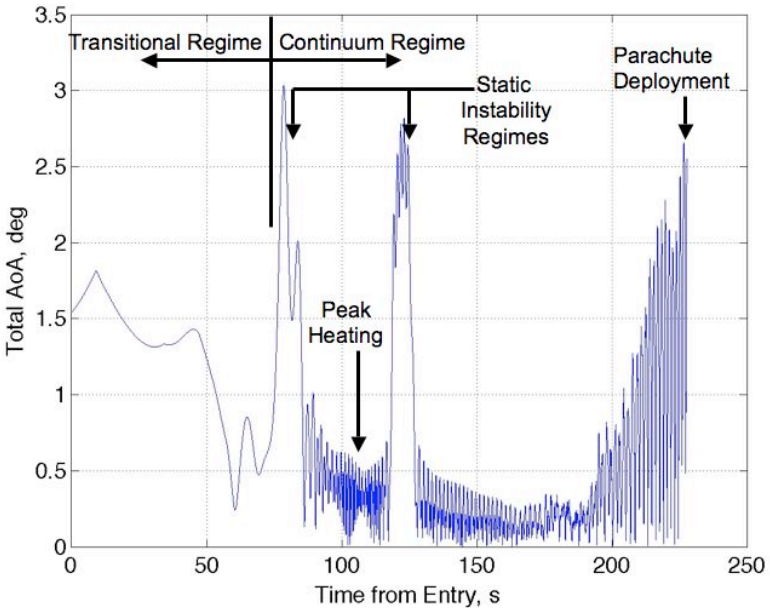

Figure 8. Nominal entry vehicle attitude through hypersonic phase of EDL.

J. Monte Carlo Dispersion Analysis

Phoenix must satisfy an array of constraints and derived requirements in order to successfully perform EDL. Trajectories are simulated and submitted through a probabilistic Monte Carlo analysis to determine the risks associated with the Phoenix descent. Some examples of performance metrics are, but are not limited to, the following observations. Phoenix must maintain within required attitude and rate deadbands for proper functionality of capsule systems. Parachute opening loads must be within set requirements for the lander and the parachute to maintain structural integrity. For all components of EDL to perform correctly, a sufficient timeline between parachute deployment and lander separation must be achieved. Requirements on parameters at landing limit the amount of vertical and horizontal velocity that the lander can endure upon landing on the surface. Of utmost importance to landing site selection is the size of the footprint, or landing ellipse, of probabilistic predicted landing latitudes and longitudes. The size of the landing ellipse determines regions of scientific interest that may or may not be achievable. Once all engineering and scientific requirements are met pre-flight, Phoenix can successfully demonstrate another entry, descent, and landing on the surface of Mars.

To assess the performance metrics and robustness of the Phoenix EDL system, a Monte Carlo analysis is performed where uncertainties are placed on many trajectory parameters. The atmosphere and wind profiles that were discussed in Subsection E are large contributors to the dispersion analysis. The largest single dispersion affecting the landing ellipse size is the entry state expected after the final TCM. The design requirement on the inertial flight-path angle at atmospheric entry is –13.0º ±0.2º. Another large contributor to landing ellipse is the calculated uncertainties on the aerodynamics. Table 1 lists the specified dispersions on the entry capsule aerodynamic database. Dispersions on the terminal descent aerodynamics of the lander were applied as uniformly distributed multipliers. The multiplier applied to the terminal descent lander aerodynamic axial coefficient C_A was dispersed from 0 to 1, while the multipliers applied to the remaining forces, C_N, C_Y, and aerodynamic moments C_m and C_n during terminal descent were uniformly distributed from –2 to 2.

Table 1. Capsule Aerodynamic Uncertainties in the Monte Carlo Analysis

Flight Regime	Coefficients	3-σ Uncertainty	Distribution
Free Molecular (Kn > 0.1)	C_A C_N, C_Y C_m, C_n C_{ll}	±5% ±0.01 (Adder), ±20% (Multiplier) ±0.005 (Adder), ±20% (Multiplier) 1.24e-6	Normal
Hypersonic Continuum (Kn < 0.001, M > 10)	C_A C_N, C_Y C_m, C_n C_{ll}	±3% ±0.01 (Adder), ±20% (Multiplier) ±0.002 (Adder), ±20% (Multiplier) 1.24e-6	Normal
Supersonic Continuum (Kn < 0.001, M < 5)	C_A C_N, C_Y C_m, C_n C_{ll}	±10% ±0.01 (Adder), ±20% (Multiplier) ±0.005 (Adder), ±20% (Multiplier) 1.24e-6	Normal
Free Molecular/Hypersonic Dynamics (M > 6)	C_{mq}, C_{nr}	±0.15	Normal
Supersonic Dynamics (M<3)	C_{mq}, C_{nr}	-50% to 100% (Multiplier), 0 to 0.1 (Adder)	Normal/ Uniform

In addition to atmospheric density, wind, state, and aerodynamic uncertainties, dispersions were placed upon entry and lander mass properties (mass, CG, moments of inertia, propellant imbalance), thruster performance, tip-off rates from cruise stage separation (CSS) and lander separation (LS), IMU model dispersions, radar performance, digital elevation map (DEM) terrain features, and ground slopes. Values for some of these dispersions are shown in Table 2. The dispersions on the IMU model, radar, DEM, and terrain slope are included in the simulation, but are not discussed further.

Table 2. Additional Applied Monte Carlo Dispersions (*indicates uniform distribution)

	Mean	3-σ value
Entry Parameters		
CSS tip-off roll rates, deg/s	0	0.1*
CSS tip-off pitch rates, deg/s	0	0.75
CSS tip-off yaw rates, deg/s	0	0.75
Mass, kg	569.7	0.5
CGx, m	1.07	0.0006
CGy,m	1.65E-04	4.02E-04
CGz, m	8.02E-05	2.14E-03
Ixx	293.15	5%
Iyy	184	5%
Izz	208.02	5%
Ixy	0.451	100%
Ixz	-4.424	100%
Iyz	0.372	100%
Lander Parameters		
LS tip-off roll rates, deg/s	0	0.5*
LS tip-off pitch rates, deg/s	0	9
LS tip-off yaw rates, deg/s	0	9
CGx, m	1.15	0.0006
Cgy, m	-6.13E-04	3.87E-04
CGz, m	0.0009	0.009
Ixx	231.25	5%
Iyy	145.81	5%
Izz	169.2	5%
Ixy	0.283	100%
Ixz	-4.204	100%
Iyz	0.333	100%
RCS Isp, s	190	20*
RCS Thrust, N	6.44	0.33
TCM Isp, s	212.5	12.5*
TCM Thrust, N	30.25	1.41

K. Monte Carlo Results

Statistical analysis using a Monte Carlo approach was performed on the Phoenix EDL scenario. Using the dispersions outlined in the previous sections, sets of 2000 trajectories were run to determine the robustness of the EDL system and its sensitivities. The results shown are based on the design requirements from a Monte Carlo analysis performed in April 2008 just prior to the start of the EDL operations phase. Performance indicators show that the lander system remains within all design requirements. Thermal parameters during the hypersonic entry indicate that the aeroheating is also within system requirements. The maximum convective heat rate during the hypersonic phase is 46 ±2 W/cm^2 (Fig. 9a), while the heat load throughout the hypersonic phase is 2390 ±140 J/cm^2 (Fig. 9b). The maximum angle of attack during peak heating is 0.6° ±0.9° (Fig. 9c), while the entry deceleration is 9.3 ±0.8 g (Fig. 9d). The requirements in the hypersonic phase for heating were set at 64 W/cm^2 for maximum convective heat rate, 3320.0 J/cm^2 for total integrated heat load, and 13.0 g for peak deceleration. In this Monte Carlo, all 2000 cases successfully met these requirements.

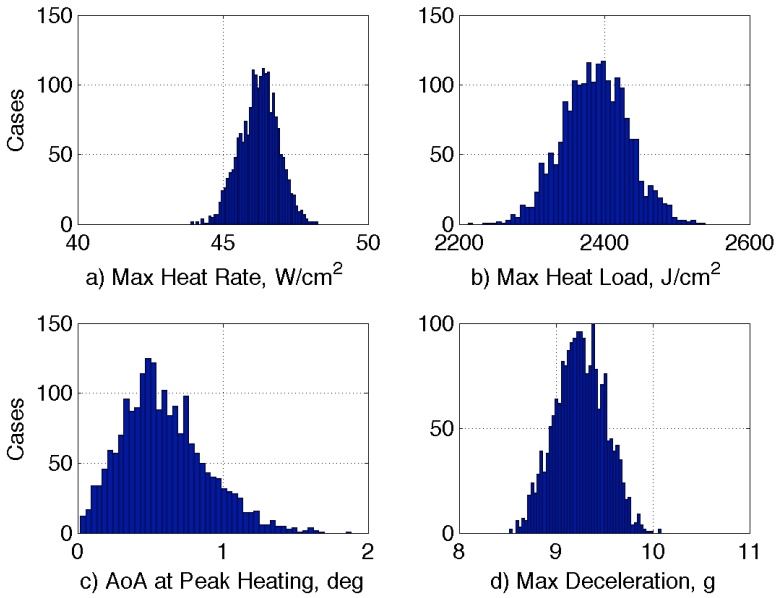

Figure 9. Hypersonic phase Monte Carlo statistics.

Key parameters in EDL performance are also obtained at parachute deploy. Figure 10 shows the parachute deployment dynamic pressure and Mach number. The parachute trigger is optimized to a mean dynamic pressure at deployment of 490 N/m^2. This mean value restricts the upper limit on dynamic pressure at deployment to reduce risk of lander structural integrity issues resulting from high parachute opening loads. The upper limit of dynamic pressure at parachute deployment is 560 N/m^2 with a lower limit of 300 N/m^2. Every case in this Monte Carlo set successfully deployed within these limits. Similarly, the Mach number was constrained to be within 1.1 < Mach < 2.1, and every case in the 2000 case Monte Carlo set fell within this criteria.

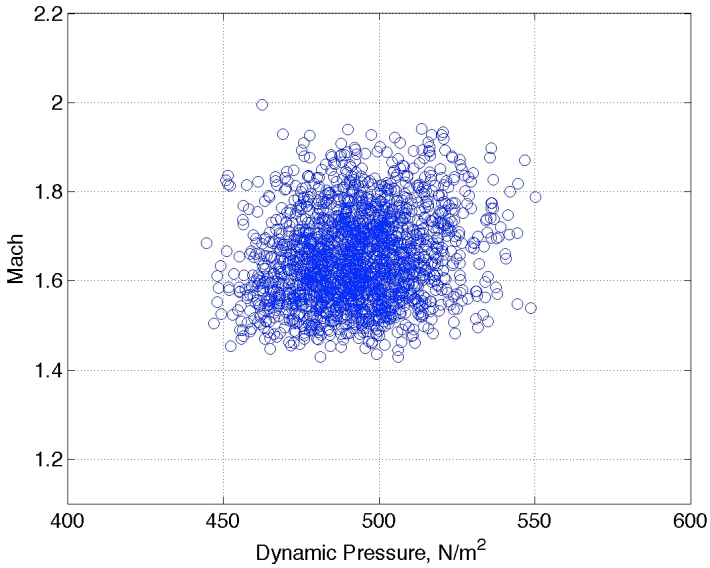

Figure 10. Dynamic pressure and Mach at parachute deploy.

The attitude at parachute deployment was of concern considering that the attitude deadbands were increased during the hypersonic phase. In the Monte Carlo, there were 38 cases out of 2000 in which the RCS thrusters fired between atmospheric entry and parachute deployment. In all 38 cases, the firings occurred just seconds prior to mortar fire. This Monte Carlo showed capsule angles of attack of 2.3° ±4.6°. The maximum angle of attack at parachute deploy was 11.3°. It was desired to keep these angles to a minimum; the limit for the angle of attack at parachute deployment was 10°. In this case, the maximum angle of attack case was the only parameter that violated this requirement. Additional key parameters at parachute deployment are velocity and altitude. The planet relative velocity at parachute deploy was 371 m/s with a 3-σ standard deviation of 60 m/s. Similarly, the altitude variation of deployment above the surface was 12.8 ±3.7 km. These altitudes are sufficiently high such that there is enough time on the parachute for reducing the velocity prior to lander separation. The length

of time on the parachute was 174 ±53 s. The minimum time on parachute was 122 s, still above the designed requirement.

Once the radar is activated, the spacecraft prepares for lander separation. Figure 11 shows the altitude above ground level (AGL) and velocity at lander separation. This figure is typically referred to as the "hockey stick" plot since there is a sharp bend in the data points due to a minimum altitude allowed for lander separation. One of the parameters that was closely monitored was the attitude rates at lander separation. This single-body simulation identified 27 cases out of 2000 that violated the 100 deg/s criteria at lander separation. As mentioned in the previous section, this high number of violation cases was not seen in the identical Monte Carlo run through the more realistic multi-body dynamical simulation.[9] Therefore, the single-body Monte Carlo results with the 27 reported violations in attitude rates at lander separation was deemed conservative. In addition, there were requirements for attitude rates at heat-shield jettison and at leg deployment both constrained at 100 deg/s, which were never violated.

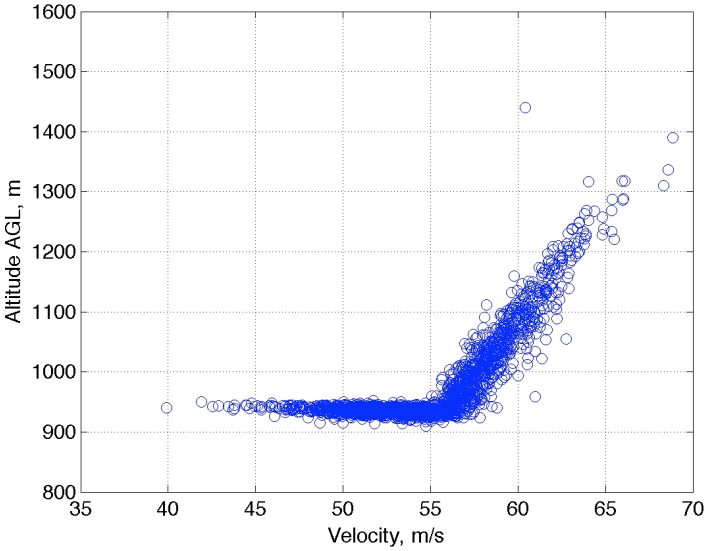

Figure 11. Altitude and velocity at lander separation.

The POST2 EDL simulation was terminated at touchdown of the three lander legs on the surface of Mars. The lander was required to satisfy velocity requirements at touchdown to be considered successful. The horizontal velocity was restricted to speeds below 1.4 m/s. Thirteen cases in this Monte Carlo violated this constraint. Vertical velocity is bounded by 1.4 m/s on the low end and 3.4 m/s on the upper end. Two trajectories violated the high vertical velocity limit, 20 cases violated the lower limit. A scatter plot of vertical and horizontal velocities is shown in Fig. 12.

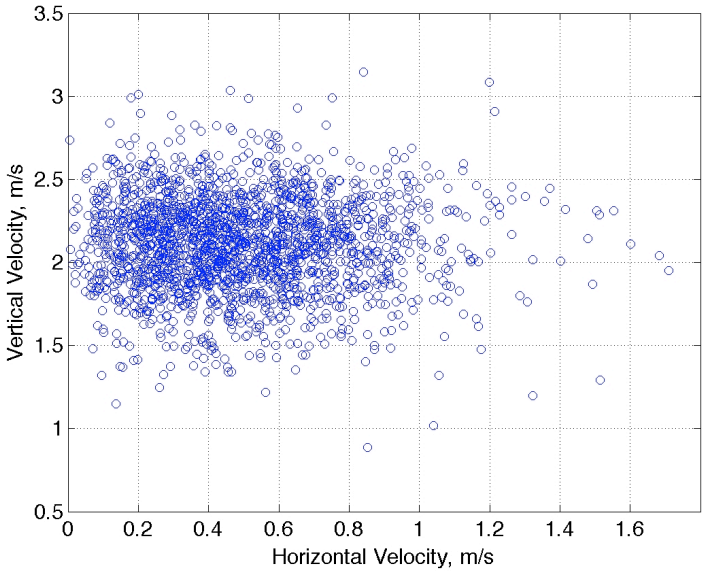

Figure 12. Touchdown velocities.

Figure 13 depicts the landing ellipse of the 2000 trajectories from the Monte Carlo set. A topographic map of the landing location referenced to the MOLA aeroid is shown in the background. The blue ellipse contains 99% of the Monte Carlo landing locations and is 103 km by 20 km in size, which is the design landing requirement. The mean landing location is indicated by the blue circle. The target location is indicated by the black x, and for reference, the actual landing site of Phoenix is shown as the red diamond. Table 3 summaries all the EDL metrics and the number of cases that violated each requirement. Note, a few weeks prior to the start of the EDL operations phase, the target location was shifted to the southeast to 68.151° north Latitude and 233.975° east Longitude.

The Monte Carlo analysis described is a baseline to which other sensitivities and trade studies were compared. The number of violations (~3%) for this single-body analysis is within expectations for the behavior of this lander and the team's understanding of the EDL system. Thousands of additional Monte Carlo analyses were performed since the Phoenix Scout mission proposal and the statistical analysis continued throughout the EDL operations phase.[6]

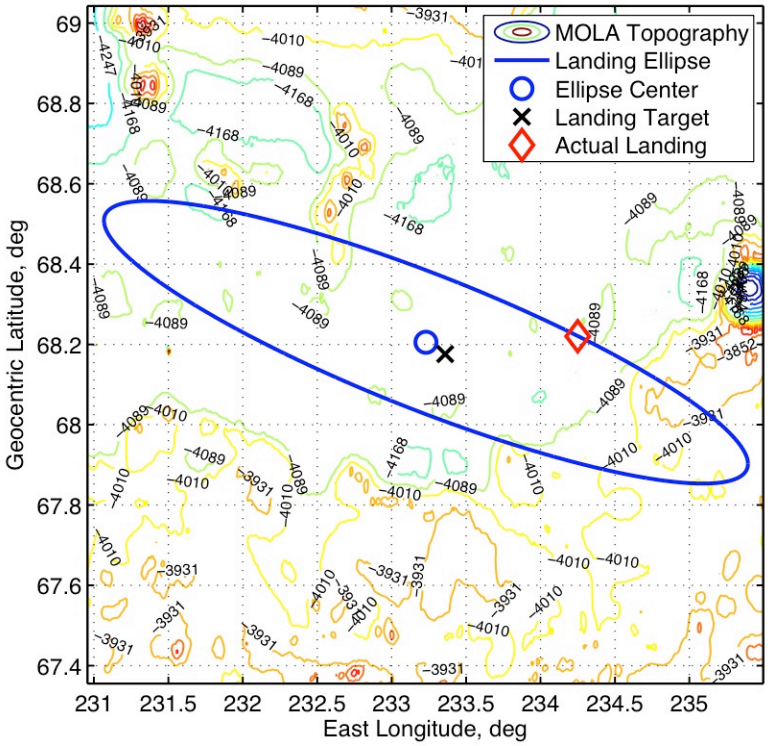

Figure 13. Predicted landing ellipse for Phoenix.

Table 3. Total Violations for Baseline Monte Carlo

Total Violations of EDL Requirements	59

Hypersonic Parameters	Violations
Peak Heat Rate < 64 W/cm2	0
Integrated Heat Load < 3320.0 J/cm2	0
AoA at Peak Heating < 10.0 deg	0
Peak Decelerleration < 13 g	0
Parachute Phase Requirements	
300 Pa< Deploy Dynamic Pressure < 560 Pa	0
1.1 < Deploy Mach < 2.1	0
Deploy Angle of Attack < 10.0 deg	1
Mach at Heatshield Jettison < 0.8	0
Rates at Leg Deploy < 100.0 deg/s	0
Terminal Descent Requirements	
Rates at Lander Separation < 100.0 deg/s	27
Propellant Usage> 5% margin	0
1.4 m/s < Touchdown Vertical Velocity < 3.4 m/s	22
Touchdown Horizontal Velocity < 1.4 m/s	13

V. Summary

Mars Phoenix landed successfully on May 25, 2008 in the northern arctic region of Mars. The entry, descent, and landing (EDL) phase of the Phoenix mission was comprised of an unguided, ballistic, hypersonic entry; deployed on a heritage disk-gap-band parachute; and propulsively completed its terminal descent phase using thruster firings for a soft landing on the surface of Mars. To ensure mission success, the robustness of this EDL scenario was assessed through a detailed simulation, which incorporated various system models. The simulation modelled events from ten minutes prior to cruise stage separation until touchdown. Monte Carlo statistical analysis of the EDL trajectory design was performed. Results from the baseline Monte Carlo are presented. The behavior of Phoenix EDL system is within requirements with very few violations.

Acknowledgments

The authors would like to acknowledge the contributions of the entire Phoenix EDL team at the Jet Propulsion Laboratory (Doug Adams, Erik Bailey, Gene Bonfiglio, Jim Chase, Curtis Chen, Ben Cichy, Dan Eldred,Richard Kornfeld, Paul Laufer, Mike Lisano, Rob Manning, Tim Priser, Dana Runge, Dara Sabahi, David Skulsky, Cris Windoffer), at Lockheed Martin Space Systems (Tim Gasparrini, Brad Haack, Mark Johnson, Tim Linn, Tim Priser, Jay St Pierre), and at NASA Langley Research Center (Jody Davis, Artem Dyakonov, Chris Glass, Karl Edquist, Ray Mineck, John Van Norman) for the overall success of the Phoenix landing. A portion of this research was carried out at the Jet Propulsion Laboratory, California Institute of Technology, under a contract with the National Aeronautics and Space Administration. Reference herein to any specific commercial product, process, or service by trade name, trademark, manufacturer, or otherwise, does not constitute or imply its endorsement by the United States Government or the Jet Propulsion Laboratory, California Institute of Technology.

References

[1] Queen, E. M., Cheatwood, F. M., Powell, R. W., Braun, R. D., Edquist, C. T. "Mars Polar Lander Aerothermodynamic and Entry Dispersion Analysis". Journal of Spacecraft and Rockets, 0022-4650 vol.36 no. 3. Pp 421-428.

[2] Cruz, M. I., Chadwick, C. "A Mars Polar Lander failure assessment". AIAA-2000-4118. AIAA Atmospheric Flight Mechanics Conference, Denver, CO Aug 14-17 2000.

[3] Shotwell, R. "Phoenix – The First Mars Scout Mission (A Midterm Report)". 57th International Astronautical Congress, Valencia, Spain Oct 2-6 2006. IAC-06-A3.3.02.

[4] Grover, M. "Overview of the Phoenix Entry, Descent, and Landing System Architecture", AIAA-2008-7213, Proceedings of AIAA Guidance, Navigation, and Control Conference bit, Honolulu, HI, August 2008.

[5] Portock, B. "Navigation Challenges of the Mars Phoenix Lander Mission", AIAA-2008-7214, Proceedings of AIAA Guidance, Navigation, and Control Conference bit, Honolulu, HI, August 2008..

[6] Prince, J. L., Desai, P. N., Queen, E. M., Grover, M. R., "Entry, Descent, and Landing Operations Analysis for the Mars Phoenix Lander", AIAA-2008-7349, Proceedings of AIAA Guidance, Navigation, and Control Conference bit, Honolulu, HI, August 2008.

[7] Broome, J., Prince, J. "Potential Entry Guidance Modifications to Improve Landing Accuracy for the 2007 Phoenix Mars Mission" AAS 2005 Guidance and Control Conference, Breckenridge, Colorado. February 5-9, 2005.

[8] Dyakonov, A., Glass, C., Desai, P. "Aerodynamic Interference Effects Due to Reaction Control System for the Mars Phoenix Entry Capsule", AIAA-2008-7220, Proceedings of AIAA Guidance, Navigation, and Control Conference bit, Honolulu, HI, August 2008.

[9] Queen, E., Desai, P., Prince, J., "Multibody modelling and Simulation for Mars Phoenix Lander Entry, Descent, and Landing", AIAA-2008-7347, Proceedings of AIAA Guidance, Navigation, and Control Conference bit, Honolulu, HI, August 2008.

[10] Brauer, G. L, Cornick, D. E., Stevenson, R. "Capabilities and Applications of the Program to Optimize Simulated Trajectories (POST)" NASA CR-2770, Feb. 1977.

[11] Braun, R. D., Powell, R. W., Engelund, W., C., Gnoffo, P. A., Weilmunster, J., K., Mitcheltree, R. A., "Mars Pathfinder Six-Degree-of-Freedom Entry Analysis," Journal of Spacecraft and Rockets. Vol 32, No. 6. November-December 1995, pp993-1000.

[12] Desai, P., N., Schoenenberger, M., and Cheatwood, F. M. "Mars Exploration Rover Six-Degree-of-Freedom Entry Trajectory Analysis" Journal of Spacecraft and Rockets, Vol 43, No 5, September-October 2006, pp. 1019-1025.

[13] Tamppari, L., J. Barnes, E. Bonfiglio, B. A. Cantor, A. J. Friedson, A. Ghosh, M. R. Grover, D. Kass, T. Z. Martin, M. T. Mellon, T. Michaels, J. R. Murphy, S. Rafkin, M. D. Smith, G. Tsuyuki, D. Tyler, and M. J. Wolff (2008), The Atmospheric Environment Expected for the Phoenix Landed Season and Location, *J. Geophys. Res.,* doi:10.1029/2007JE003034, in press

[14] Edquist, K., Desai, P., Schoenenberger, M. "Aerodynamics Prediction for the Mars Phoenix Entry Capsule", AIAA-2008-7219, Proceedings of AIAA Guidance, Navigation, and Control Conference bit, Honolulu, HI, August 2008.

[15] Cruz, J. R. "Mars Science Laboratory Supersonic Parachute Data" MSL-366-0637 Rev A. July 21, 2004 [unpublished]